NUMERICAL INVESTIGATIONS OF FATIGUE CRACK GROWTH IN SHAFTS

Angelo R Maligno,
Research Fellow, University of Nottingham, UK

Ramesh Chandwani
Managing Director, Zentech International Ltd., UK

Chris Timbrell
Principal Engineer, Zentech International Ltd., UK

THEME

3D Crack Simulation – Fracture Mechanics

KEYWORDS

Fatigue crack growth, FEA, Notches.

SUMMARY

Numerical modelling of three dimensional (3D) non-planar fatigue crack growth under mixed mode conditions represent a crucial factor in fracture mechanics in order to assess the residual life of components. This paper focuses on developing a damage tolerance approach that can be used for the design of aeroengine shaft components under the general mixed-mode loading conditions in the presence of stress-raising features. The initial work has validated numerical results against crack growth measurements on uniaxial tensile specimens under Mode-I loading. Then, more realistic loading scenarios have been applied on shafts to investigate the influence of different parameters (e.g. crack orientation) on fatigue crack growth. All of the present work is based on linear elastic fracture mechanics approaches, including the Paris and Walker theories.

NUMERICAL INVESTIGATIONS OF FATIGUE CRACK GROWTH IN SHAFTS

1. Introduction

The research presented in this paper is part of a broader study which aims to develop a numerical and experimental methodology to simulate fatigue crack growth in shafts. In particular, while the “initial crack” in numerical models can be easily introduced [1], in experimental tests this represents a challenging issue. Preliminary studies have been carried out to study the effects of micro-notches in uniaxial tensile specimens. Results from these investigations (e.g. proper loading conditions, initial crack shape) have been used in FE analyses of hollow shafts. In addition, the reliability of numerical results based on remeshing methods using the commercial code ZENCRACK has been proved in [2, 3], in which numerical results have been validated against experimental data on CT specimens and solid shafts.

2. Material

Super CMV (S/CMV) is a medium carbon high strength alloy steel with the main elements of Chromium, Molybdenum and Vanadium. The development of the material has been achieved by using the CMV which is already in market. The high strength is obtained using lower tempering temperature; the fatigue properties were improved by introducing a triple vacuum melting procedure to improve the cleanness of the material and finally the strength of the material was improved by changing the composition of the material. After these alterations the material is capable of working at elevated temperatures and also under high forces and was named as S/CMV. This particular material has been introduced to reduce the weight of the main shafts as it has a very high percentage of nickel, allowing the material to work under elevated temperatures. This material is high in strength and has fatigue resistance. Elements in this material give high strength and resistance against fatigue as they are the main factors for the application.

3. Methodology

The numerical modelling of three-dimensional (3D) non-planar fatigue crack growth under mixed mode conditions represents a crucial factor in fracture mechanics in order to assess the residual life of components. The numerical studies are based on finite element (FE) analyses using the remeshing approach. This study employs ZENCRACK for automated 3D remeshing and crack propagation calculations along with ABAQUS as the finite element solver. ZENCRACK is a 3D crack analysis tool able to read in an uncracked finite element model and to produce a cracked finite element model. Stress intensity factors or the energy release rate are calculated automatically from the results of the cracked finite element analysis. Furthermore crack growth can be undertaken by extending the crack position. An updated finite element model is then created and run to simulate crack growth (Figure 1).

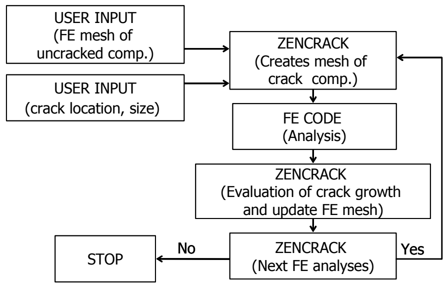

Figure 1: Flow chart for crack growth prediction analysis [1].

It is well known that linear elastic fracture mechanics provides a method for describing the stress at a crack front. Three modes of local behaviour are used to define the opening, sliding and tearing stress intensity factors, K_I, K_{II} and K_{III} respectively. These can be combined to obtain an equivalent energy release rate term, *Geq* [4, 5]:

$$Geq = \frac{1}{\overline{E}}\left(K_I^2 + K_{II}^2\right) + \frac{1}{2G}\left(K_{III}^2\right) \tag{1}$$

where $\overline{E} = E/(1-\nu^2)$ for 3D problems. In order to determine new crack front positions, the crack propagation direction (CPD) must be computed. Although expressions exist to calculate the crack growth angle based upon the stress intensity factors, ZENCRACK adopts an alternative method based on the maximum energy release rate at a crack front point. The *G*-criterion states that a crack will grow in the direction of maximum energy release rate. The CPD, $\theta = \theta_o$, is then determined by:

$$\left(\frac{dG}{d\theta}\right)_{\theta=\theta o} = 0 \; ; \quad \left(\frac{dG}{d\theta}\right)^2_{\theta=\theta o} \leq 0 \tag{2}$$

In the present work, *G* is computed using the virtual crack extensions method (VCE) [6]. The application of a series of virtual crack extensions ultimately generates a growth angle at the crack front node that, in the general case, may be out-of-plane.

In the present work the Walker equation has been used to describe the fatigue crack growth:

$$\frac{da}{dN} = C_o\left[\Delta K_R (1 - R)^{(n-1)}\right]^m \tag{3}$$

where: *a* = crack size; N = number of fatigue cycles; C_o, n, m = material constants (subscript ***o*** refers to values at R=0); ΔK = stress intensity factor range = K_{max} - K_{min}; R = stress ratio. The material constants have been experimentally [2, 3, 4] determined by testing CT specimens of S/CMV at different load ratios. The determined parameters for the Walker equation are: C_o=2.8646E-12**;** m=2.5612 and n=0.41. The critical K_{IC} has been also experimentally [2,3,4] evaluated: $\mathbf{K_{IC}}$=2890.32 MPa(mm)$^{0.5}$

3.1 Topological approach

The approach that has been adopted by ZENCRACK to model the details of the crack region is based on the use of 'crack-blocks'. ZENCRACK has two types of crack-blocks [1]:

(a) - Standard crack-blocks
- The standard crack-blocks reduce to a single element on their back faces and merge with the rest of the mesh via shared nodal numbers (Figure 2).
- The crack-blocks consist of "through" and "quarter circular" crack blocks.

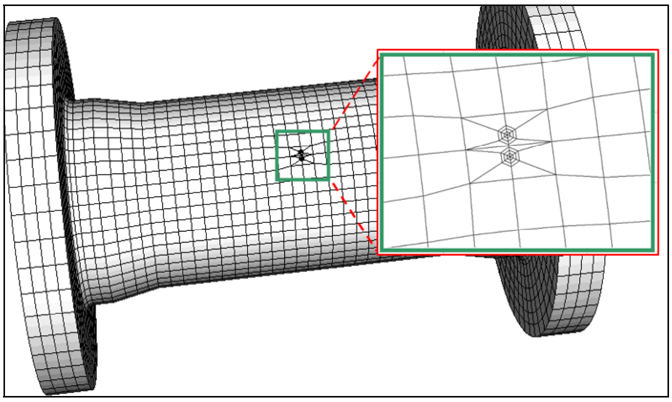

Figure 2: Example of standard crack-blocks

(b) - Large crack-blocks
- The large crack-blocks contain multiple nodes on their back faces and are used with surface-based tying to connect them to the surrounding (dissimilar) mesh (Figure 3).
- The crack-blocks consist of "through" and "quarter circular" crack blocks.

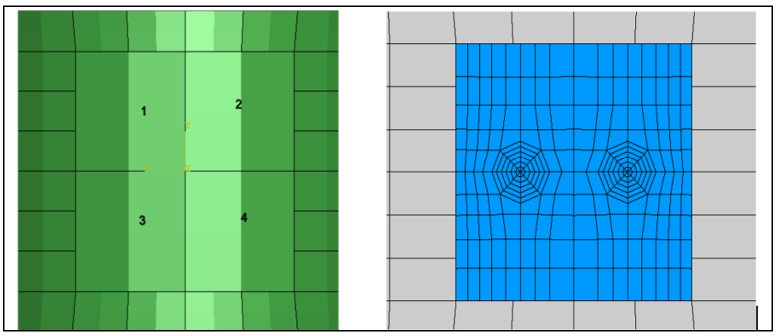

Figure 3: Example of large crack-blocks

4. Results

4.1 Uniaxial tensile specimen

This research deals with the development of a numerical and experimental methodology, to simulate fatigue crack growth in shafts under mixed-mode loadings. For planned future tests on lab-scale shafts a micro-notch will be machined on the outside surface. Hence, it is necessary to determine the micro-notch influence on crack initiation and especially whether it can be considered an 'initial crack'. Experimental tests on uniaxial tensile specimen (Figure 4a) have been carried out to assess the effects of the following parameters on crack initiation: micro-notch shape, micro-notch dimensions, loading conditions.

The micro-notch has been micro-machined using a milling tool 0.2mm in diameter that will produce a slot of 0.2mm thick (Figure 4b). The maximum depth is 0.5mm (Figure 4c). The diameter of the specimen is 4.0mm in the 'cracked' region (Figure 4a).

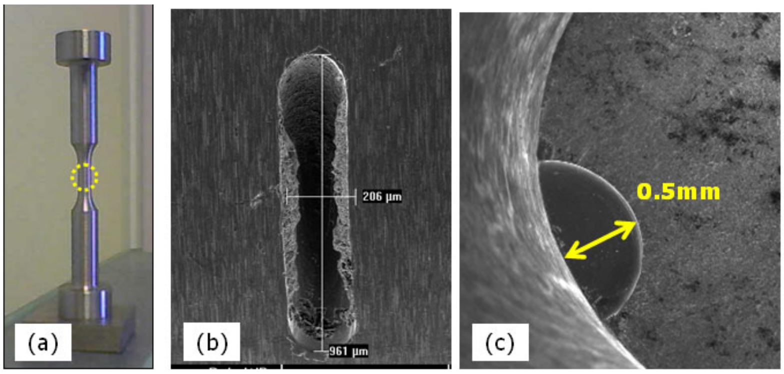

Figure 4: Uniaxial tensile specimen (a) & details (b, c) of machined micro-notch

Experimental tests have been performed on specimens with micro-notch depths of 0.4mm and 0.5mm. The calculated stress concentration factor (Roark's formulas), introduced by the micro-notch suggests the application of a loading stress such that the ratio of applied stress and yield stress should be:

$$\Sigma = \frac{\sigma_{applied}}{\sigma_Y} \leq 0.8 \qquad (4)$$

Experimental tests have confirmed the analytical calculations and, in order to avoid a drastic failure within a few cycles (<500), a cyclic loading stress of 1000MPa (yield stress for the S/CMV: $\sigma_Y = 1242$MPa) is applied at different loading ratios, namely: R=0.1, R=0.3, R=0.5, R=0.7. The final data of experimental tests and numerical computations are presented in Table-1. Experimental and numerical data show a good agreement for R ratios 0.1 and 0.3 for the two different crack lengths (0.4mm and 0.5mm) under investigation.

It has been seen that regions of plasticity-induced crack closure, probably due to the notch influence zone (NIZ) [7], are likely to be detected for loading ratios R>0.3.

The crack progression (experimental tests and numerical computation) is displayed in Figure 5, where the transition from the slow crack growth to the catastrophic final failure (dashed line in Figure 5b) in the uniaxial specimen has been determined with scanning electron microscope (SEM) techniques. In Figure 5 it is evident the similarity of experimental and FE analyses to predict the final drastic failure in which $K_I=K_{IC}$.

The influence of different initial crack geometries (semi-elliptical and semi-circular) has been numerically investigated. The FE results (Table-2), have been compared to analytical solutions related to the through-thickness crack growth for solid shafts [8]. The terms *a* and *b* in Table-2 are the semi-major and semi-minor axes of the ellipse, respectively. An example of compared computational and analytical data is depicted in Figure 6.

Data	R ratio	Initial crack length range [mm]	Final crack length [mm]	Cycles to failure (N)
Experimental	0.1	0.4	NA	7560
	0.1	0.5	~2.0	4220
	0.3			8517
	0.5			20370
	0.7			130380
Zencrack	0.1	0.4	1.76	7043
		0.5	2.05	4650
	0.3	0.4	1.76	8513
		0.5	2.05	6717
	0.5	0.4	1.76	14772
		0.5	2.05	9564
	0.7	0.4	1.76	25259
		0.5	2.05	16353

Table-1 Through thickness crack growth in uniaxial specimen

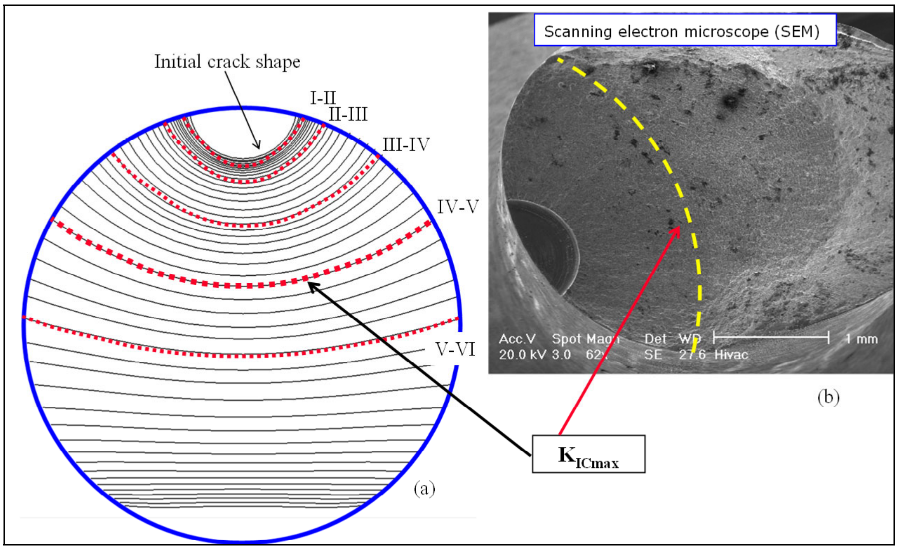

Figure 5: Crack evolution in numerical simulations (a) and experimental test (b)

b/a	Initial crack length	Final crack length	Maximum number of cycles (N)
0.6	0.4	3.74	5590
0.75			6145
1			7043

Table-2 Through thickness crack growth in uniaxial specimen with semi-elliptical initial cracks

The relationship used to describe the crack growth is equation 3, where ΔK_{th}=6.74MPam$^{0.5}$ and accounts for crack closure developments that could take place for short crack regimes; ***C***=3.36E-12**;** ***m***=2.5612. The term ΔK_{th} has been applied only in region I-II (Figure 6) in order to account for retardation factors due to the (likely) plasticity at the notch-tip [7]. ΔK_I has been calculated from equation 4, a relationship for semi-elliptical crack surfaces in shafts under tension [8], where σ is the applied stress. Parameter F_I depends on the geometry of the crack and the shaft. Its values are available in [8].

$$\frac{da}{dN} = C[\Phi(\Delta K_I) - \Delta K_{th}]^m \qquad (5)$$

$$F_I = \frac{K_I}{\sigma\sqrt{\pi b}} \qquad (6)$$

The correction factor Φ (range: 1.2-2.75) in equation (5), has been introduced as a fitting parameter to describe the crack progression in region IV-V and V-VI (Figure 6) where the ratio ***b/a*** is circa zero and it is outside the range of validity of F_I [8]. The ratio ***b/a*** has been updated throughout the analytical solution (Table-3) to match the numerical crack evolution depicted in Figure 6.

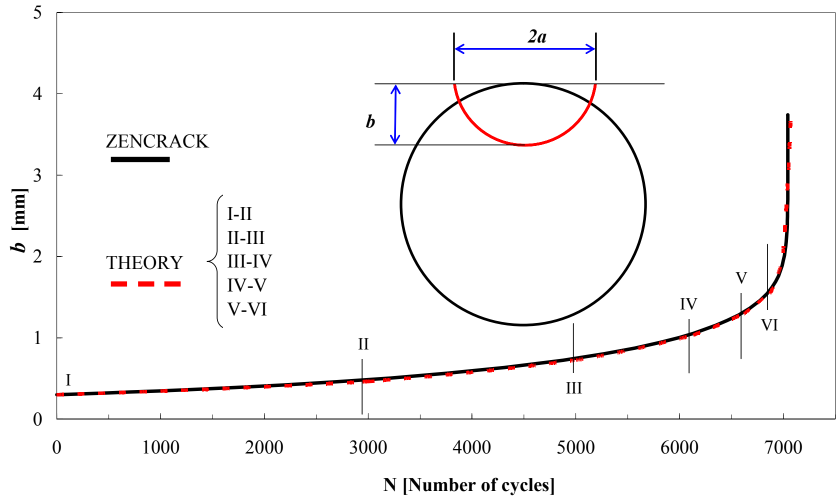

Figure 6: Trend of crack evolution (numerical and analytical comparison)

b/a	Region	Cycles
1	I-II	0
0.86	II-III	3246
0.64	III-IV	5003
0.414	IV-V	6132
0.236	V-VI	6625
~0	VI⇒	6873

Table-3 Update of *b/a* applied in the analytical solution

4.2 Shaft Components under Mixed Mode Loadings

Two different shaft features, under cyclic axial and torsion loadings, have been investigated: 1) hollow plain-shaft Figure 7(a) and 2) hollow shaft with holes Figure 7(b).

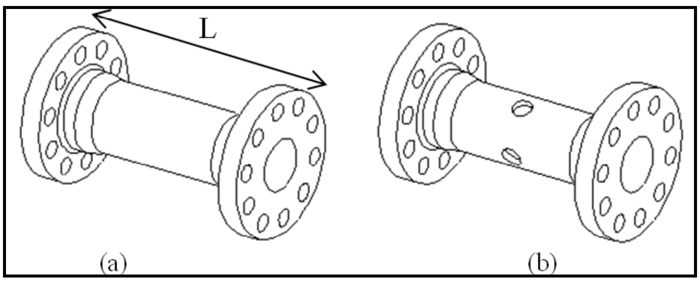

Figure 7: Shaft features

The dimensions of the shafts are: thickness = 6.0mm; outer diameter = 50.0mm; length L = 150.0mm, holes diameter = 10mm.

4.3 Hollow plain shafts

A systematic study on fatigue crack growth on aeroengines shafts with an initial crack oriented at an angle of 45^o and 90^o to the shaft axis has been carried out. An "initial crack" geometry with a semi-circular shape (part-through crack) has been considered in this research. A cyclic mixed-mode loading has been applied to numerical models: torque = **14.4kNm**; axial loading = **10.4kN**. In Figure 8 and Figure 9 numerical results from the analyses on shafts with an initial crack of 45^o and 90^o to the shaft axis have been compared. The onset of the critical stress intensity factor K_{IC} has been monitored and it is indicated in the figures.

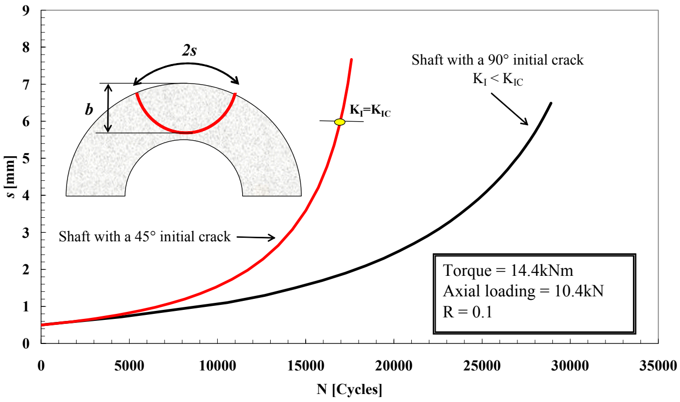

Figure 8: Crack growth in shafts with initial part-through (semi-circular) crack

It is worthwhile to note that the crack propagation in shafts with an initial crack oriented at an angle of 45^o to the shaft axis is faster than the 90^o orientation case. In fact, the maximum principal stresses, due to their orientation, tend to apply a pure Mode-I loading to the crack flanks for an initial crack direction of 45^o[3]. The effect of different torsional loading has also been investigated. The reference torque, 14.4kNm, has been incremented by 20% and 40% of the initial value. Finite element calculations (Figure 9) show a highly detrimental effect in terms of life estimation for higher values of the torque. The value of the K_{IC} at different numbers of cycles has been also monitored and it is depicted in Figure 9.

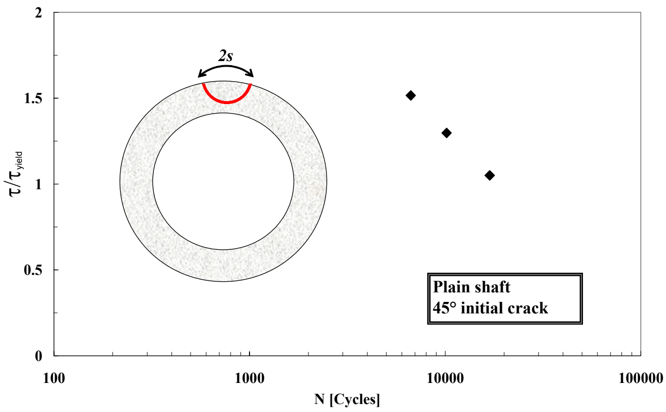

Figure 9: K_{IC} **onset for different values of torsional loading (initial crack at 45o)**

4.4 Hollow shafts with holes

Numerical analyses have been performed on hollow shafts with (two) holes in order to investigate the notch effect on fatigue crack growth. The initial crack shape is a quarter of a circle and it is oriented at an angle of 45^{o} to the shaft. The immediate consequence of the notch (hole in the shaft) is the introduction of a stress concentration factor (SCF). The value of this SCF has been evaluated using the von Mises stress:

$$SCF\,\Big|_{\text{von Mises}} = \frac{\sigma_{VM}^{Max}}{\sigma_{VM}^{nom}} = 2.48 \qquad (7)$$

Figure 10 shows the crack growth of the node on the outside surface (Node A) and the crack propagation throughout the thickness (Node B). In addition, due to the Maximum Principal Stresses distribution in the holes [3], the through-thickness crack evolution develops faster than the growth on the outside surface. Finally, the applied loading conditions lead to a very short life estimation of the shaft; in fact at lower values of R ratios (less than 0.7) only few cycles are simulated.

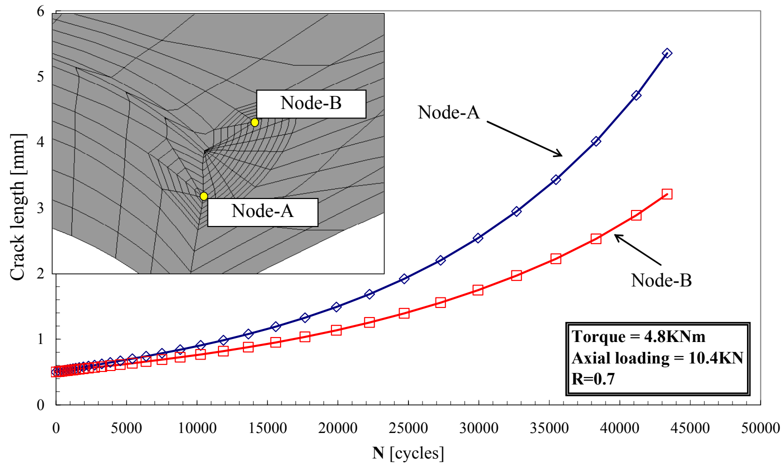

Figure 10: Crack growth on outside surface (B) & through thickness (A) in the hole

Thus, in order to achieve a more realistic life estimation, the torque has been decreased of one third of its initial value applied to the plain hollow shafts. The updated mixed-mode loading conditions are: torque = 4.8kNm; axial loading = 10.4kN. A comparison between the crack growth on the outside surface by applying the same magnitude of the torque to the plain shaft and shaft with hole is showed in Figure 11. It can be noticed that the holes introduce a detrimental effect in terms of life estimation in aeroengines shafts.

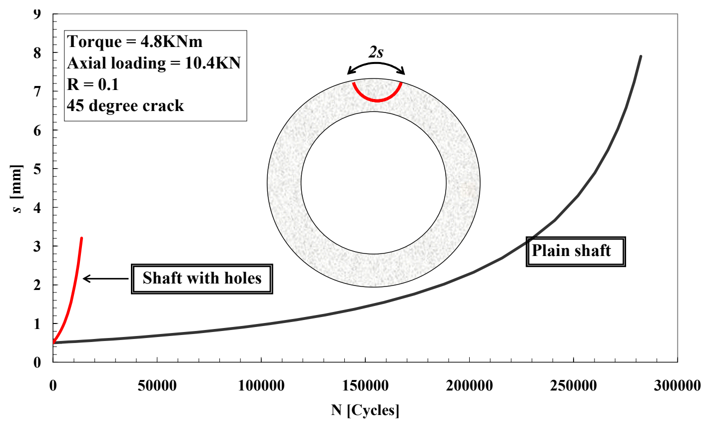

Figure 11: Crack growth on outside surface in hollow shafts with & without holes

4.5 Effect of thickness

The future test programme was planned to run experimental tests on lab-scale aeroengines shafts 6mm thick. Nevertheless, the influence of thickness on fatigue crack has been considered an important parameter worth further investigation. Therefore, hollow shafts with holes and reduced thickness (5mm) have been considered in this numerical study. FE analyses have shown that the crack growth rapidly increases in the thinner shaft. In particular both the through-thickness crack propagation (Figure 12) and the crack growth on the outside (Figure 12) surface undergo a faster crack evolution.

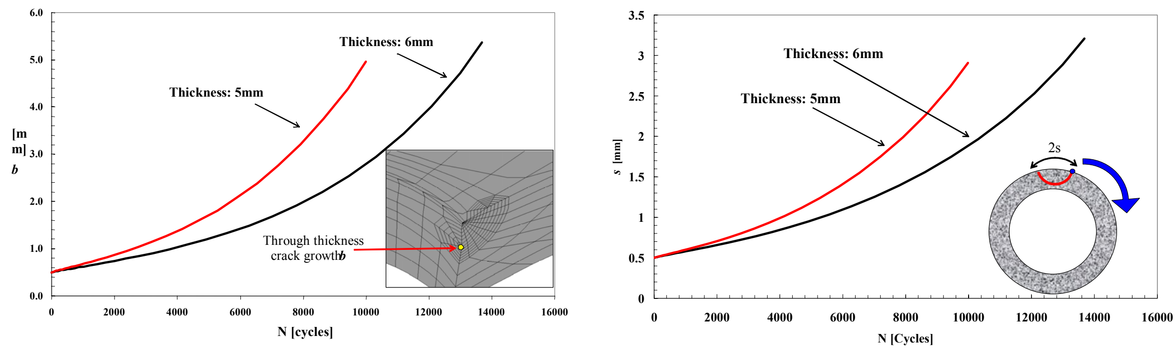

(a) Through-thickness crack growth in the hole (b) Crack growth on the outside surface

Figure 12: Effect of different thickness in crack evolution (shafts with holes)

Computational results are summarised in Table-4 and Table-5. FE analyses demonstrate that a reduction of circa 17% of the initial shaft thickness leads to an average diminution of 25.7% in terms of life estimation.

Torque	Axial loading	R	Initial crack length	Final crack length	Cycles
4.8kNm	10.4kN	0.1	0.5[mm]	5.35[mm]	13685
		0.3			17815
		0.5			25366
		0.7			43366

Table-4 Through-thickness crack growth in shafts with holes 6mm thick

Torque	Axial loading	R	Initial crack length	Final crack length	Cycles
4.8kNm	10.4kN	0.1	0.5[mm]	4.96[mm]	9981
		0.3			13316
		0.5			18956
		0.7			32414
6.7kNm		0.1			4024
10.0kNm					1471

Table-5 Through-thickness crack growth in shafts with holes 5mm thick

4.6 <u>Break-through strategy</u>

ZENCRACK is not able to automatically model the "break-through" after the semicircular crack reaches the bore (Figure 13). A used-defined crack profile can be used to overcome this issue as shown in Figure 13.

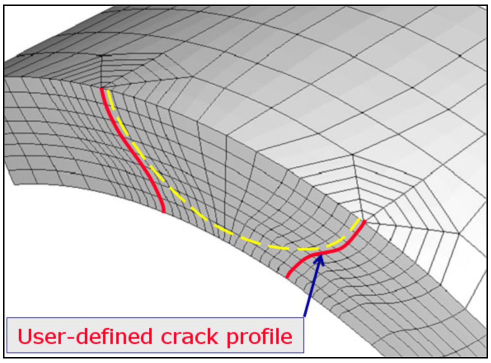

Figure 13: Ideal break-through

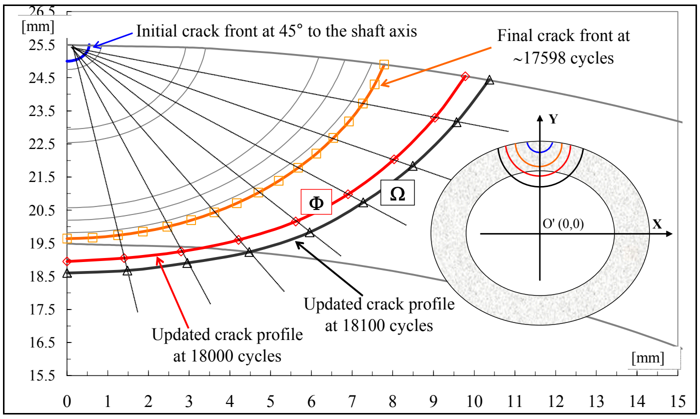

(at 45^{o} the cross-section of the shaft is an ellipse)

Figure 14: Break-through strategy

The strategy developed to create the break-through crack is achieved by extrapolating (versus the number of cycles) the nodal coordinates lying on the final crack front, reached at the end of the part-through analysis (Figure 14). Although this technique represents a viable way to extend the crack front after it reaches the shaft bore, these crack fronts (for example crack front **Φ** - Figure 14) imply new meshes with severely distorted elements which prevent the FE analyses from running. Possible solutions are:

- to create a crack front at a higher number of cycles such as the crack front **Ω** (Figure 14).
- to modify the crack front shape by smoothing sharp angles as shown (bold line) in Figure 13.

5. Conclusion

Experimental, numerical and analytical studies on uniaxial tensile specimens under fatigue loading have established the basic requirements for micro-notches to simulate initial cracks in shafts. These results have been applied in numerical aeroengine shafts to simulate fatigue crack growth under different loading conditions. FE analyses have demonstrated that the crack evolution and life estimation strongly depend on: crack orientation, loading ratio R, shaft geometry, shaft thickness and, mainly, presence of holes.

REFERENCES

[1] ZENCRACK Manual, Version 7.4

[2] R. Sabesan, S.B. Leen, E.J. Williams, Fatigue crack growth in shafts using the finite element method, Proceedings from the conference Fatigue-2007, Cambridge 2007 (UK).

[3] A.R. Maligno, S. Rajaratnam, S.B. Leen, E.J. Williams, Numerical study on fatigue crack growth in aeroengines shafts using remeshing techniques, in preparation.

[4] ABAQUS User's and Theory Manuals, Version 6.5, HKS (2005).

[5] H.G. DeLorenzi, On the energy release rate and the J-integral for 3D crack configurations, Journal of Fracture 19 (1982), 183-193

[6] D.M. Parks, The virtual crack extension method for nonlinear material behavior, Computer Methods in Applied Mechanics and Engineering 12 (1977), 353-364.

[7] F. Ding, M. Feng, Y. Jiang, Modeling of fatigue crack growth from a notch, International Journal of Plasticity 23 (2007) 1167–1188

[8] Y. Murakami, H. Tsuru, Stress-intensity factor equations for semi-elliptical surface crack in a shaft under bending, Stress Intensity Factors Handbook, Vol. II, Oxford Pergamon Press, 1987.